Optofluidic *in situ* maskless lithography of charge selective nanoporous hydrogel for DNA preconcentration

Hyoki Kim,[1] Junhoi Kim,[1] Eun-Geun Kim,[1] Austen James Heinz,[1] Sunghoon Kwon,[1,a)] and Honggu Chun[2,a)]
[1]*School of Electrical Engineering and Computer Science, Seoul National University, San 56-1, Shillim 9-dong, Gwanak-ku, Seoul 151-744, Republic of Korea*
[2]*Advanced Institutes of Convergence Technology, Seoul National University, 864-1, Iui-dong, Yeongtong-gu, Suwon, Gyeonggi-do 443-270, Republic of Korea*

(Received 8 October 2010; accepted 20 October 2010; published online 30 December 2010)

An optofluidic maskless photopolymerization process was developed for *in situ* negatively charged nanoporous hydrogel [poly-AMPS (2-acrylamido-2-methyl-1-propanesulfonic acid)] fabrication. The optofluidic maskless lithography system, which combines a high power UV source and digital mirror device, enables fast polymerization of arbitrary shaped hydrogels in a microfluidic device. The poly-AMPS hydrogel structures were positioned near the intersections of two microchannels, and were used as a cation-selective filter for biological sample preconcentration. Preconcentration dynamics as well as the fabricated polymer shape were analyzed in three-dimensions using fluorescein sample and a confocal microscope. Finally, single-stranded DNA preconcentration was demonstrated for polymerase chain reaction-free signal enhancement. © *2010 American Institute of Physics.* [doi:10.1063/1.3516037]

I. INTRODUCTION

Detection of DNA in a microfluidic environment has attracted much attention due to its substantial importance to forensic science, clinical diagnostics, and cancer research. In practice, the short path length of the microfluidic channel and small copy number of the target DNA make sensitive detection challenging. To alleviate these limitations, various techniques have been reported in a form of miniaturized system.[1–17] The conventional way to enhance the sensitivity of detection is to increase the copy number of DNA by the chemical amplification through polymerase chain reaction (PCR).[1–3] However, various components are necessary in PCR chemistry, such as enzymes and primers as well as precise temperature control. It may also be necessary to incorporate subsequent purification steps before analysis, which adds additional complications to miniaturization. One promising alternative to sensitive detection of DNA would be the capability to concentrate the sample DNA prior to the analysis without any additional chemical involvement.[4–17]

Sample preconcentration exploits various sample characteristics, including electric charge, size, mobility, and affinity.[4–17] DNA has the unique property of having a uniform charge to size ratio, making charge selective preconcentration efficient. Among the preconcentration techniques using the electric property of DNA, the electrokinetic trapping technique has received much attention due to its high sensitivity and easy miniaturization. Electrokinetic trapping usually utilizes a charged nanochannel (or nanoporous membrane) between microchannels, allowing for enrichment of counterions along the structure while excluding coions.[11–17] The local electric field gradient and concentration polarization are induced when an electric field is applied across the charged nanochannel so that sample preconcentration can be achieved.[17] The electrokinetic trap-

[a)]Author to whom correspondence should be addressed. Electronic addresses: skwon@snu.ac.kr and hongguchun@snu.ac.kr.

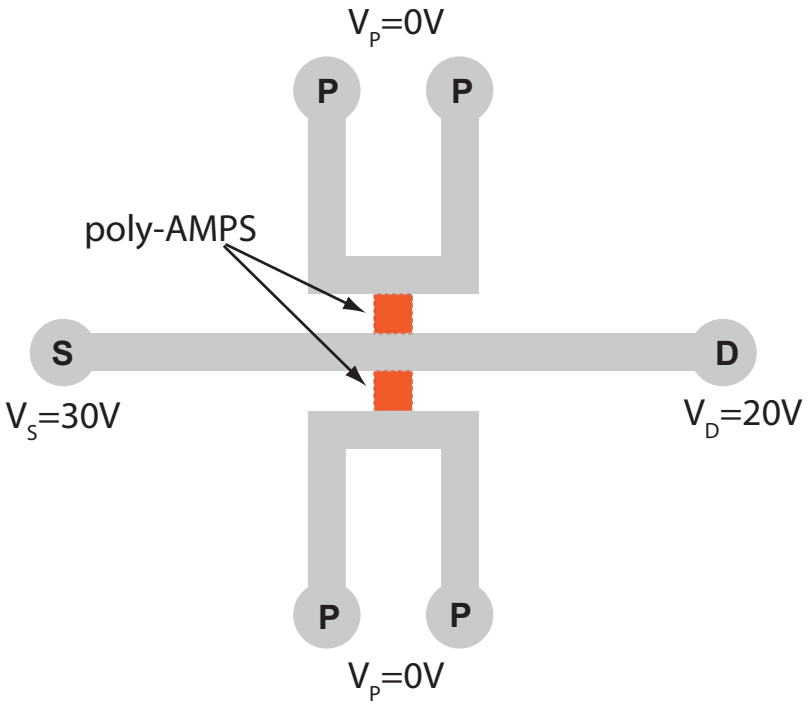

FIG. 1. Microfluidic channel design for charge selective preconcentration using negatively charged hydrogel, poly-AMPS. Charged sample flows in the main channel (S-D) and potassium phosphate buffer is filled in polymer channel (P).

ping technique does not suffer from overall device size, since the preconcentration occurs in the immediate proximity of the ion depleted boundary, and has shown a high efficiency for concentrating charged biomolecules. However, the conventional fabrication process to incorporate an ion-permselective membrane into a microfluidic device involves complex steps. For example, multistep lithography and etching steps are required for a monolithic nanochannel fabrication between microchannels[11] and the incorporation of a charged nanoporous membrane between microchannels by manual alignment does not ensure reproducible characteristics.[12] These issues stimulated research efforts for developing easy fabrication methods, which include the *in situ* charge selective nanoporous hydrogel fabrication by photopolymerization[17] (Fig. 1). However, conventional contact mask lithography may suffer from diffraction induced pattern blurring when exposing micrometer-sized pattern through the millimeter-thick glass substrate, which reduces spatial resolution [Fig. 2(a)]. This blurred UV pattern can cause main microchannel clogging as well as an unpredictable polymer boundary. Especially, the polymer boundary shape is critically important because even a minute difference in the structural design might lead to a complicated modification in terms of concentration mechanism.

Alternative approach for light exposure in a microfluidic environment includes a method based on projection lithography [Fig. 2(b)]. Previously, optofluidic maskless lithography (OFML) system has been developed to provide dynamic *in situ* polymerization in a microfluidic environment.[18–20] In the OFML, computer-controlled spatial light modulator dynamically generates arbitrary pattern of UV light, reducing complex polymerization process by doing away with the necessity of physical photomasks and mask alignment (Fig. 3). The OFML system has the unique advantage in fabricating small polymer structure through a thick substrate because the objective lens can focus the pattern at a desired depth. In addition, appropriate focal depth choice of the objective lens can ensure a vertical polymer shape in the microchannel.

In this paper, we show the effect of diffraction induced pattern blurring in the contact mask lithography and present a miniaturized biological sample preconcentration using charge selective

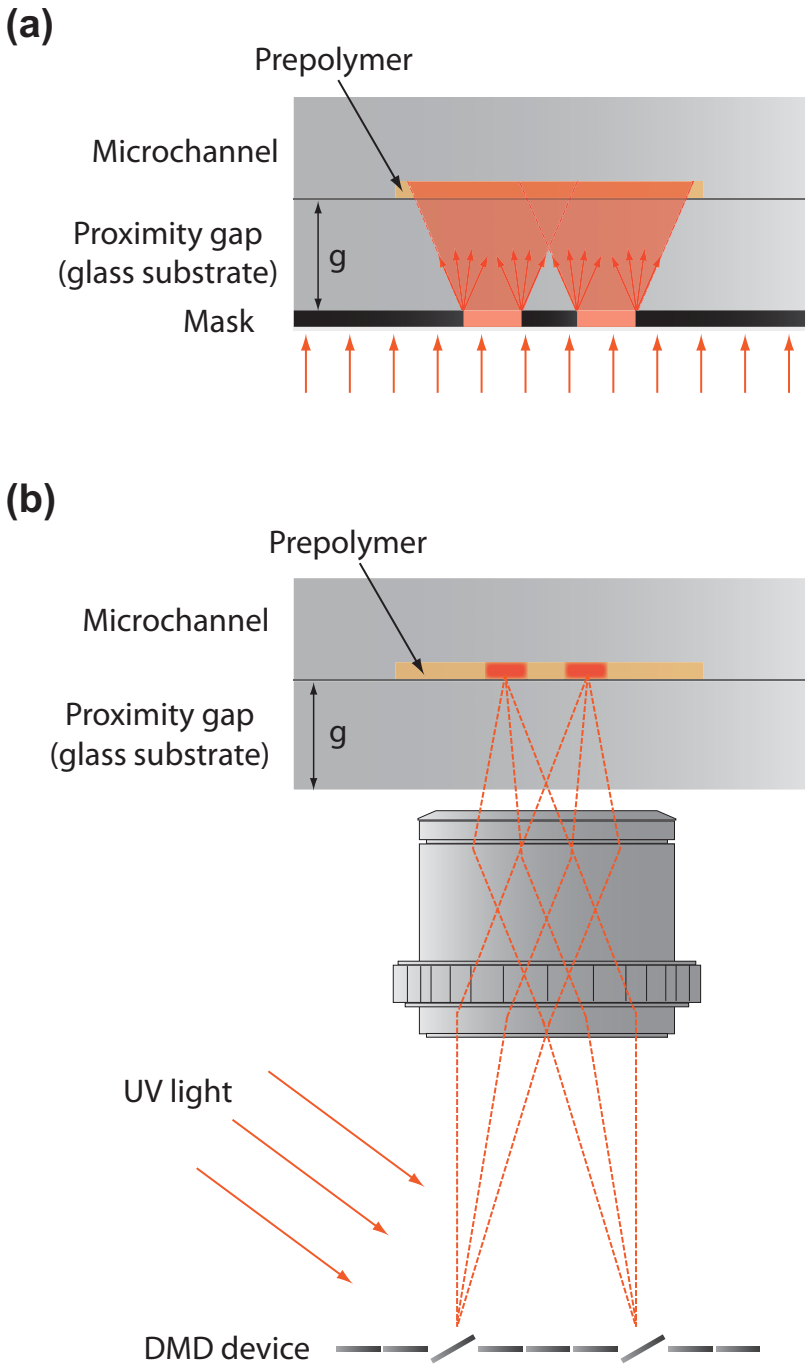

FIG. 2. (a) Schematic diagram of proximity lithography. (b) Schematic diagram of projection lithography using DMD device as a dynamic mask.

hydrogel, poly-AMPS (2-acrylamido-2-methyl-1-propanesulfonic acid) via OFML. Also, three-dimensional optical characterization of the charged hydrogel and preconcentration profile is presented.

II. MATERIALS AND METHODS

A. Reagents

2-acrylamido-2-methyl-1-propanesulfonic acid (AMPS), 2-hydroxy-4′-(2-hydroxyethoxy)-2-methylpropiophenone, *N*,*N*′-methylenebisacrylamide, 3-(trimethoxysilyl) propyl methacrylate

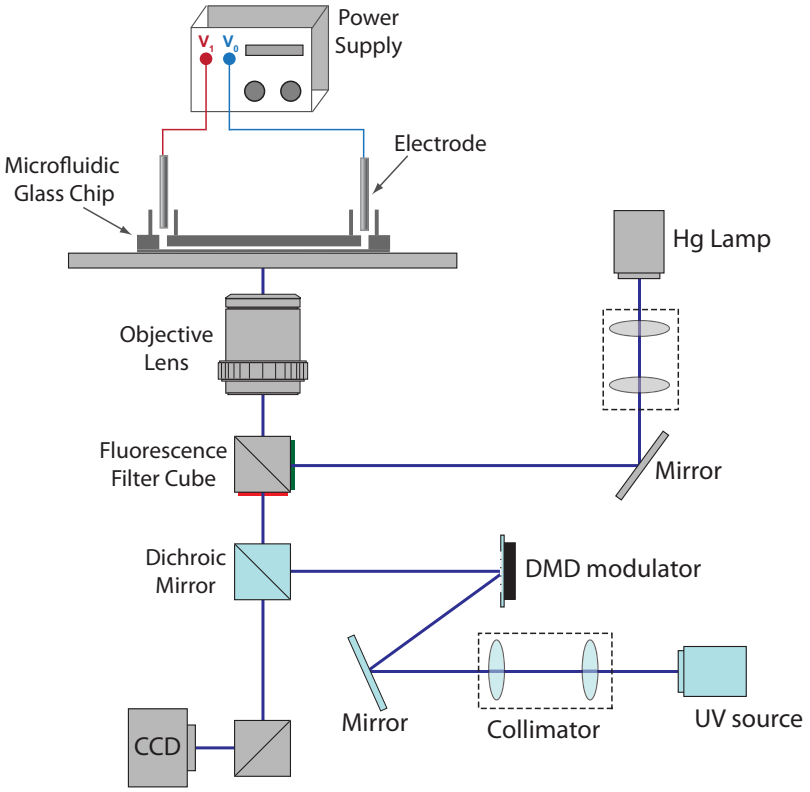

FIG. 3. Schematic illustration of instrumentation for charge selective preconcentration. A negatively charged hydrogel is produced by OFML system. Spatial light modulator (DMD) inside the system produces arbitrary UV light pattern dynamically.

(TMSMA), glacial acetic acid, potassium phosphate dibasic, and fluorescein disodium salt were purchased from Sigma-Aldrich (St. Louis, MO, USA). Ethyl alcohol, isopropyl alcohol (IPA), potassium chloride (KCl), hydroquinone (HQ), and sodium hydroxide (NaOH) were purchased from Daejung Chemicals (Korea). All materials were used as received without further modification. De-ionized (DI) water was prepared using Milipore's filtration system (Billerica, MA, USA). Fluorescent oligomer (sequence: 5′-Cy3-GAA GTT GTA GAG TGT-3′) was purchased from IDT (Commercial Park Coralville, IA, USA). Buffer solutions were 20 mM phosphate buffer at *p*H 9.3 unless otherwise stated. We used 100 nM Cy3 labeled DNA solution in 0.1× TE buffer (1 mM Tris, 0.1 mM EDTA, 20 mM NaCl, and 0.05% SDS) for the preconcentration analysis.

B. Diffraction pattern simulation

To show the issue of pattern blurring of the contact mask lithography, we calculated a light intensity profile based on the Fresnel diffraction algorithm using a custom program written in MATLAB 7 (The MathWorks, Natick, MA).[21] Plane wave of 365 nm wavelength is exposed to a mask with two adjacent 10 μm holes separated by 50 μm, and then, a light intensity profile was calculated 1 mm away from the mask.

C. Microfluidic chip fabrication

Fabrication of glass microfluidic chip was based on the previous work.[17] The devices were fabricated by standard photolithography and wet etching on 0.9 mm thick glass substrate, followed by thermal bonding to seal the microfluidic channels. The dimensions of the microfluidic channel are 50 μm (width) and 12 μm (height).

D. OFML system

Schematic illustration of OFML system is shown in Fig. 3. The system includes optical microscope with fluorescence filter cubes (IX71, Olympus), UV source (200 W, mercury-xenon lamp, Hamamatsu) and digital mirror device (DMD) (discovery 1100 chipset, Texas Instrument). UV light from the UV source passes through a beam collimator, prior to redirection by the DMD. The pattern of UV light is controlled by a DMD with self-designed computer program, which synchronizes the pattern of DMD and the incident UV light. Patterned UV light travels through the side port of the microscope and reflects off a dichroic mirror. The pattern of UV light is focused by passing through the objective lens after which point it exposes on a given substrate of interest. Size of a micromirror in DMD is 13.68 μm$\times$13.68 μm, so the calculated ideal resolution of each micromirror after focusing is $\sim$0.7 μm when using 20$\times$ objective lens with numerical aperture (NA) of 0.45.

E. Poly-AMPS fabrication

Prior to the fabrication of poly-AMPS, TMSMA is coated inside the microfluidic channel to covalently link the substrate and the poly-AMPS. 200 μl of TMSMA is diluted with 500 μl of DI water and 300 μl glacial acetic acid. The microfluidic channel is filled with the dilute TMSMA mixture for 3 min in dark environment, then washed with IPA and dried. The monomer solution for poly-AMPS fabrication is prepared with 2 M AMPS in DI water, 2 wt % 2-hydroxy-4′-(2-hydroxyethoxy)-2-methylpropiophenone, 2 wt % N,N'-methylenebisacrylamide, and 200 ppm HQ. The monomer solution is flowed into the microfluidic channel, and then UV pattern generated by OFML system is exposed to the microfluidic channel where the monomer solution was filled. Patterned UV light with energy of 6.8 W/cm^2 is exposed through the 20$\times$ objective lens (Olympus, NA=0.45). After polymerization, the microchip is washed with a 1*M* KCl solution.

F. Chip manipulation

0.1 N NaOH was flowed through each microchannel for 3 min to enhance electro-osmotic flow. Two power supplies (IT 6720, Itech and E3633A, Hewlett Packard) are used for voltage application via Pt electrodes.

G. Optical system

Optical micrographs are acquired by a true-color charge coupled device camera (DP71, Olympus) which is directly aligned to the inverted microscope (IX71, Olympus) with a high pressure mercury lamp. Three-dimensional (3D) fluorescent micrographs are acquired using a confocal microscope (CTR6500, Leica).

III. RESULTS AND DISCUSSION

First, the calculated diffraction pattern of the contact mask lithography is shown in Fig. 4. The result shows that the UV exposure through the 10 μm hole causes significant pattern blurring at a distance of 1 mm from the mask. When this blurred pattern is exposed over the microchannel network for the *in situ* polymerization as shown in Fig. 1, the main microchannel is easily clogged. The channel clogging can be prevented by controlling the UV exposure time. However, the gradual intensity UV pattern does not produce a sharply defined polymer boundary, shape, and size, which are critical requirements for reproducible electrokinetic characteristics and corresponding concentration polarization process for the DNA preconcentration. In contrast, the 3D morphology of the poly-AMPS structure produced by the OFML system is analyzed using a confocal microscope. To characterize this, we inject the monomer solution into the microfluidic channel, and expose the patterned UV light of 50 μm by 100 μm within a wide-open region of the channel. The polymerized structure has a height of 12 μm, the same height of the microchannel. After polymerization, uncured monomer solution is washed with 1*M* KCl solution, then the

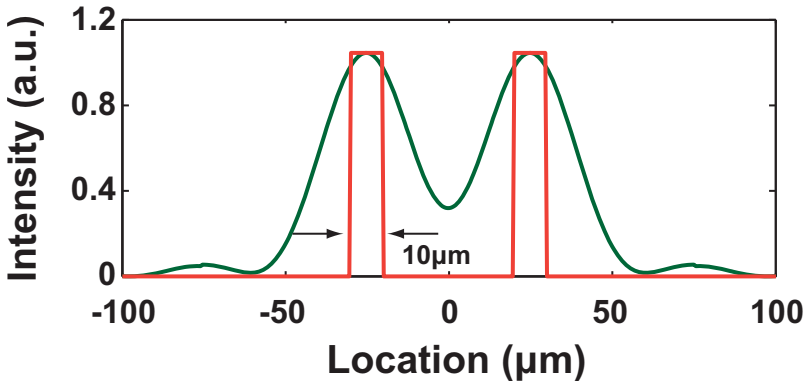

FIG. 4. Calculated intensity of light passing through the contact mask (red line: mask opening with feature size of 10 μm, green line: Fresnel diffraction pattern at the distance of 1 mm from the mask).

solution of 10 μM fluorescein sodium salt in 20 mM phosphate buffer at *p*H 7.4 is added to the channel opening. The negatively charged fluorescein molecule cannot diffuse into the negatively charged poly-AMPS network, which allows us to monitor the 3D morphology via confocal microscope. Transmission microscope image and the corresponding vertical cross section image of the polymeric structure are shown in Fig. 5. The 3D fluorescent confocal microscope image reveals that the polymer structure produced by OFML system has a sharply defined boundary. In addition, the size of the polymer is highly reproducible according to the exposure pattern. The OFML system with the chosen NA of the objective lens provides sufficient depth of field in a confined channel with 12 μm height, resulting in a vertical wall profile.

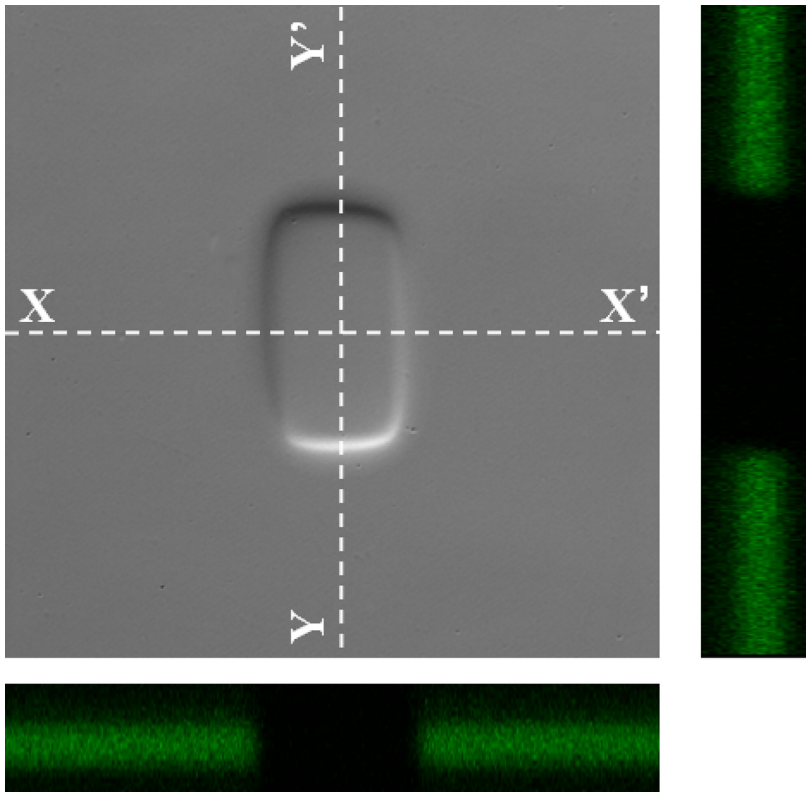

FIG. 5. 3D optical characterization of a negatively charged hydrogel produced by the OFML system.

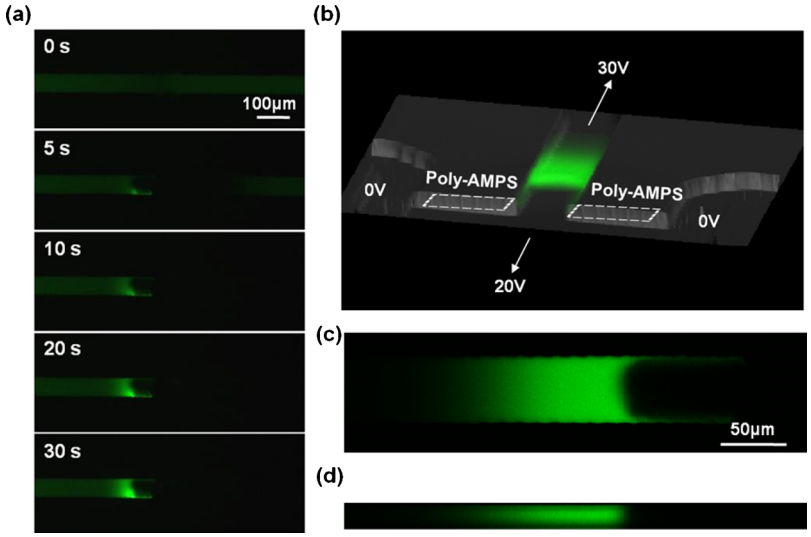

FIG. 6. 3D characterization of sample preconcentration. Negatively charged fluorescein molecule is used for analysis. (a) Time dependent sample preconcentration profile. (b) 3D confocal microscope image after 1 h of preconcentration. (c) Top view of preconcentration profile (b). (d) Cross sectional side view of (b).

Design of the microfluidic chip for the preconcentration of the charged molecule is shown in Fig. 1. Using the OFML system, we produced two poly-AMPS structures in the polymer channel (P) adjacent intersection with the main channel (S-D). In order to measure the concentration of fluorescent molecules, 10 μM fluorescein sample is loaded into the main channel (S-D), while buffer solution is loaded into the polymer channel (P). Fluorescein solution flows through the main channel when voltage is applied to both channel ends. Detailed explanation of the preconcentration mechanism can be found in previous work.[17] Briefly, when P reservoirs are grounded to 0 V, cations are selectively extracted through the negatively charged hydrogel, and anions expelled from the area near the negatively charged hydrogel. As a result, an ion-depleted region develops between the two hydrogel plugs. Along the ion-depleted region, the electric resistance and corresponding electric field substantially increase. Therefore, electrophoretic force (EP) is locally strengthened at the ion-depletion region. Near the ion-depletion region, the direction of anion EP is the opposite of the EOF of the main channel, thus anions entering the ion-depleted region experience an enhanced EP that drives back toward the sample reservoir. Consequently, anions are stacked to the left of the ion-depletion boundary where the main channel flow rate and EP balances each other.

To characterize the local concentration of charged molecules in our device, we applied 30 V at the sample reservoir (S), 20 V at the drain reservoir (D), and 0 V at the polymer reservoirs (P). The concentration dynamics is shown in Fig. 6(a). One can see the local concentration of negatively charged fluorescein increases as time passes. 3D optical characterization performed after 1 h of preconcentration via confocal microscope [Figs. 6(b)–6(d)] clearly illustrates an increase of the fluorescein concentration prior to the ion-depletion region at the channel intersection. Figure 6(c) is a horizontal cross section of the concentrated region. Concentration of the fluorescein is highest near the ion-depletion region and decreases as the location approaches to the sample reservoir (S). Figure 6(d) is the vertical cross section of the concentrated region. A 3D fluorescence image reveals that the local concentration of the charged molecule is highest at the center of the vertical channel and the profile is symmetric across entire 50 μm width of the microchannel. The preconcentration process is stable even after 1 h of accumulation.

Lastly, we demonstrate the preconcentration of the DNA. 100 nM Cy-3 labeled single stranded oligonucleotides of 15 base pairs in 0.1× TE buffer mixture is flowed into the main channel (S-D). We applied 40 V at the sample reservoir (S), 5 V at the drain reservoir (D), and 0

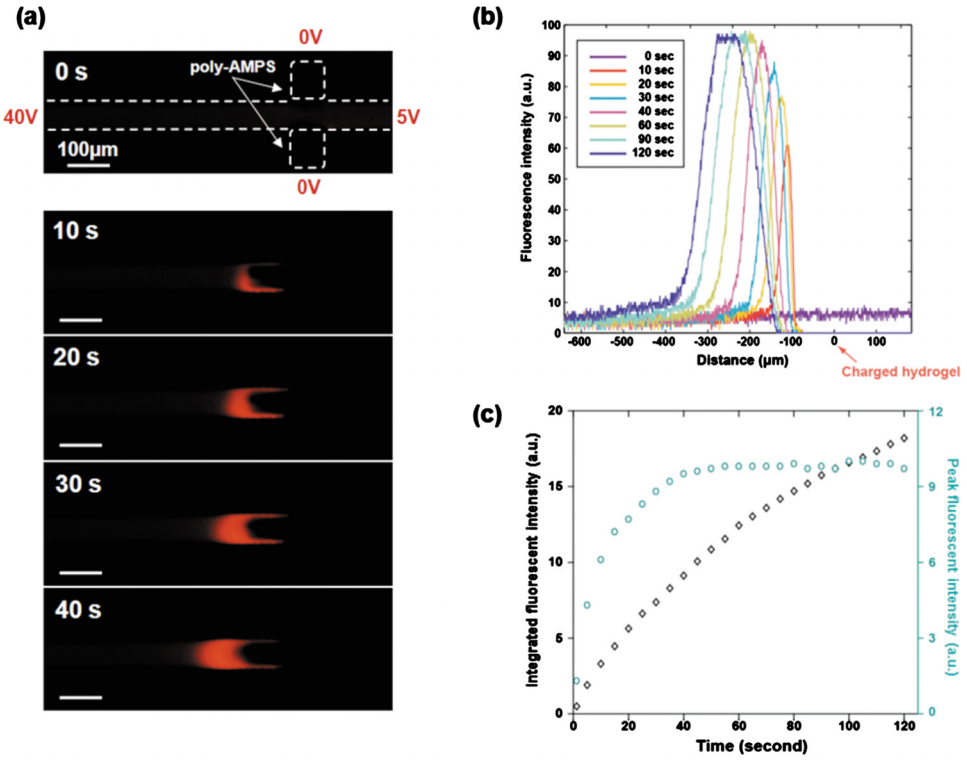

FIG. 7. Preconcentration profile of DNA. Cy-3 labeled 15 bp ssDNAs are concentrated in the region near the ion-depletion region. (a) Time dependent sample preconcentration profile. (b) Fluorescence intensity across the main microchannel (S-D). Distance is referenced to the left corner of the poly-AMPS plug. (c) (left *y*-axis) Integrated fluorescence intensities over the entire preconcentrated plugs, (right *y*-axis) peak fluorescence intensities of preconcentrated plugs.

V at the polymer reservoirs (P). The dynamics of the DNA concentration are shown in Fig. 7(a). At time zero, before the voltage application, fluorescence signal is very weak. However, a strong fluorescent signal is detected at the left side of the ion-depleted region after the application of voltage. The spatial distribution of the local concentration along the main channel at the center can be seen in the Fig. 7(b). The fluorescence intensity increases linearly for 20 s and then levels off, showing saturation after 40 s (up to ~50-fold). However, the size of accumulated plug increases, keeping preconcentration rate constant [Fig. 7(c)]. The result reveals that DNA can be rapidly and effectively concentrated using the OFML-based charged nanoporous hydrogel system.

IV. CONCLUSION

We developed a high resolution polymer fabrication method based on the OFML system for *in situ* charge selective nanoporous hydrogel fabrication in a glass microchannel. Confocal microscope analysis of a charge selective hydrogel, poly-AMPS, showed sharply defined boundary and vertically even wall structure, enabling stable electrokinetic trapping for preconcentration of DNA. The preconcentration process was characterized on a microfluidic device incorporating a pair of poly-AMPS using anion samples, fluorescein. Additionally, the developed system showed highly efficient single-stranded DNA (ssDNA) preconcentration for subsequent analysis. The fabrication process for the device presented here is simple, fast, and reproducible providing an efficient way to concentrate low copy number DNA for subsequent analysis or use.

ACKNOWLEDGMENTS

This work was partly supported by the IT R and D program of MKE/KEIT (10030573, Development of Photonic CMOS based Intelligent Silicon Bead) and the Korea Science and Engineering Foundation (KOSEF) grant funded by the Korean government (MEST) (Grant No.

2010-0017860), G1010-001 and G1010-002 funded by Gyeonggi-do, Industrial Strategic technology development program (10037410, Development of Next Generation DNA Sequencer) funded by the Korea government (MKE), and Hi Seoul Science/Humanities Fellowship from Seoul Scholarship Foundation.

[1] J. Khandurina, T. E. McKnight, S. C. Jacobson, L. C. Waters, R. S. Foote, and J. M. Ramsey, Anal. Chem. **72**, 2995 (2000).
[2] J. S. Marcus, W. F. Anderson, and S. R. Quake, Anal. Chem. **78**, 956 (2006).
[3] E. T. Lagally, I. Medintz, and R. A. Mathies, Anal. Chem. **73**, 565 (2001).
[4] A. Guttman, Anal. Chem. **71**, 3598 (1999).
[5] J. Khandurina, S. C. Jacobson, L. C. Waters, R. S. Foote, and J. M. Ramsey, Anal. Chem. **71**, 1815 (1999).
[6] M. Hsieh, W. Tseng, and H. Chang, Electrophoresis **21**, 2904 (2000).
[7] A. Wainright, U. T. Nguyen, T. Bjornson, T. D. Boone, Electrophoresis **24**, 3784 (2003).
[8] D. Liu, M. Shi, H. Huang, Z. Long, X. Zhou, J. Qin, and B. Lin, J. Chromatogr., B **844**, 32 (2006).
[9] J. Astorga-Wells, S. Vollmer, T. Bergman, and H. Jörnvall, Anal. Chem. **79**, 1057 (2007).
[10] C. Kuo, J. Wang, and G. Lee, Electrophoresis **30**, 3228 (2009).
[11] Y. Wang, A. Stevens, and J. Han, Anal. Chem. **77**, 4293 (2005).
[12] K. Zhou, M. L. Kovarik, and S. C. Jacobson, J. Am. Chem. Soc. **130**, 8614 (2008).
[13] D. Stein, Z. Deurvorst, F. H. J. van der Heyden, W. J. A. Koopmans, A. Gabel, and C. Dekker, Nano Lett. **10**, 765 (2010).
[14] T. Hahn, C. K. O'Sullivan, and K. S. Drese, Anal. Chem. **81**, 2904 (2009).
[15] J. Dai, T. Ito, L. Sun, and R. M. Crooks, J. Am. Chem. Soc. **125**, 13026 (2003).
[16] P. Kim, S. J. Kim, J. Han, and K. Y. Suh, Nano Lett. **10**, 16 (2010).
[17] H. Chun, T. D. Chung, and J. M. Ramsey, Anal. Chem. **82**, 6287 (2010).
[18] S. E. Chung, W. Park, H. Park, K. Yu, N. Park, and S. Kwon, Appl. Phys. Lett. **91**, 041106 (2007).
[19] S. E. Chung, W. Park, S. Shin, S. Ah Lee, and S. Kwon, Nature Mater. **7**, 581 (2008).
[20] H. Kim, J. Ge, J. Kim, S. Choi, H. Lee, H. Lee, W. Park, Y. Yin, and S. Kwon, Nat. Photonics **3**, 534 (2009).
[21] K. Abedin, M. Isla, and A. Haider Opt. Laser Technol. **39**, 237 (2007).